Localization and modeling of reaction and diffusion to explain folate behavior during soaking of cowpea

Fanny Coffigniez[a], Michael Rychlik [b, c], Christine Sanier[d], Christian Mestres [a], Lisa Striegel [b]
Philippe Bohuon[e], Aurélien Briffaz [a*]

Journal of Food Engineering

[a] UMR Qualisud, CIRAD, univ Montpellier, TA B-95/16, 73 rue J-F. Breton, F- 34398 Montpellier cedex 5, France

[b] Chair of Analytical Food Chemistry, Technical University of Munich, Alte Akademie 10, 85354 Freising, Germany

[c] Centre for Nutrition and Food Sciences, Queensland Alliance for Agriculture and Food Innovation, The University of Queensland, Coopers Plains, QLD 4108, Australia

[d] CIRAD, PHIV, UMR AGAP TA 108/02, 73 rue J-F. Breton, F- 34398 Montpellier cedex 5, France
AGAP, Univ Montpellier, CIRAD, INRA, Montpellier SupAgro, Montpellier, France.

[e] UMR QualiSud Food Process Engineering research unit, Montpellier SupAgro, univ Montpellier, 1101 av. Agropolis, B.P. 5098, F-34093 Montpellier cedex 5, France

* Corresponding author: Aurélien Briffaz, CIRAD, UMR Qualisud, TA B-95/16, 73 rue J-F. Breton,F-34398 Montpellier cedex 5, France Tel: +33 4 67 61 59 13; Fax: +33 4 67 61 44 49. E–mail address: aurelien.briffaz@cirad.fr

Abstract

A first modelling approach was used to understand the behaviour of folate in cowpea seeds during soaking at different temperatures (30 °C, 60 °C and 95 °C). Folic acid, 10-formylfolic acid, 5-methyltetrahydrofolate, and 5-formyltetrahydrofolate were quantified in both the seeds and the soaking water during the process. A 2D-axisymmetric seed soaking simulator was then built considering these 4 folate vitamers to simultaneously describe diffusion, oxidation and interconversion of the single vitamers. The model adjustments revealed the predominance of folate diffusion at 60 °C and 95 °C (apparent diffusivity 2-3×10^{-11} $m^2.s^{-1}$) whereas at 30 °C enzymatic interconversions of all vitamers into 5-methyltetrahydrofolate were observed (reaction rate of 8.0×10^{-5} s^{-1} for 5-formyltetrahydrofolate). The results of this study allow us to recommend a preliminary soaking step to retain folate in seeds and to improve the bioavailability of folates for human nutrition.

Keywords

Folates; legume; diffusion; reaction kinetics; soaking; interconversion.

1. Introduction

Today, the growing world population together with climate change threaten global food security (Tscharntke et al., 2012). In this context, consuming legumes rather than meat would be more sustainable for the environment (De Boer and Aiking, 2011) thanks to their capacity to fix nitrogen in the soil (Graham and Vance, 2003) and their lower water requirements for growth (Crews and Peoples, 2004). In terms of nutritional value, legumes are rich in essential nutrients including proteins (around 25%) which contain several essential amino acids (lysine, leucine, and phenylalanine), starch (50-60%), but also minerals (potassium, calcium, zinc, iron) and vitamins (lutein, niacin, thiamine, pyridoxine, folate, ascorbic acid) (Iqbal, Khalil, Ateeq, & Khan, 2006; El-Adawy, 2002; Gonçalves et al., 2016).

In this study, we focus on folate content (B9 vitamin) in cowpea, a legume widely grown and consumed in West Africa. Folates are present in different forms in the seeds, mainly polyglutamates partially bound to starch and protein (Arcot and Shrestha, 2005) and/or being methylated or formylated (Scott, Rébeillé, & Fletcher, 2000; Rébeillé et al., 2006). Folates play an important role in the synthesis of purine and methionine in plants (Gorelova et al., 2017). Depending on the country, the daily recommended folate intake ~~is~~ varies between 200 and ~~300~~ 400 µg for adults (Krawinkel et al., 2014). Hoppner & Lampi, (1993) showed that cowpea seeds represent a significant source of folates since they contain 367.1 µg/100 g (db), compared to other legumes such as pea seeds (282.0 µg/100g (db)) (Ringling & Rychlik, 2012). Since folate bioavailability strongly depends on food structure and composition, synthetic folic acid which is fully bioavailable has been chosen as a reference, allowing to define a dietary folate equivalent (DFE, expressed in µg) (Suitor and Bailey, 2000). Therefore, the consumption of 120 g of cowpea seeds could almost fulfil the daily requirement for adults with a DFE of about 260 µg.

For consumption, legume seeds often require a long soaking step prior to cooking. A soaking-cooking process can destroy sensitive nutrients including folates and hence needs to be controlled. Indeed, Hefni & Witthöft, (2014) showed a 32% reduction in total folate content in *Faba* bean after boiling for 30 min, 90% of which was lost in the soaking water. Nevertheless, the same authors reported a 50% increase in folate content after a soaking at room temperature for 12 h, probably due to germination. Combining a soaking step at room temperature for 16 h and a boiling step for 2 h caused a 53% reduction in total folate in chickpea and a 46% reduction in pea (Dang et al., 2000). Clearly, the choice of an appropriate soaking-cooking temperature is determinant in preserving or promoting total folate content in the seeds. Since they have different bio-availability (5-methyltetrahydrofolate (5-CH_3-H_4folate) being the most bioavailable for the human organism), the different folate vitamers need to be quantified separately which has only been done by a few authors (Rucker et al., 2001).

There are only a few models in the literature that mechanistically describe the way the folate behaves during the soaking-cooking of legumes. Delchier et al., (2014) used the Fick equation to describe the diffusion of folates during the cooking of spinach and green beans. Oey et al., (2006) and Viberg et al., (1997) modelled 5-CH_3-H_4folate oxidation assuming a first order kinetic reaction in a liquid medium. However, to the best of our knowledge, no available model describes folate oxidation and conversion coupled to diffusion. Many authors already reported the enzymatic interconversion between the different forms in plants (Rébeillé et al., 2006; Jägerstad and Jastrebova, 2013), but the possible presence of this reaction scheme during the soaking process has not yet been studied.

The aim of this study was thus to elaborate a mass balance of the different forms of folates in cowpea seed and in the soaking water during soaking at 30 °C, 60 °C and 95 °C and to establish the diffusive and reactive (degradation or production) fractions. The diffusion of folates was observed by immunostaining the 5-CH_3-H_4folate in seeds during soaking-cooking process. Our results will make it possible to recommend how to retain folate in cowpea seeds during the soaking-cooking process.

2. Materials and methods

2.1. Material

The cowpea cultivar used in the study was the *Wankoun* brownish variety provided by IITA Benin. It was purchased in September 2017. The seeds were kept in a vacuum pack and stored at 4 °C in the dark until use.

2-(N-morpholino)-ethanesulfonic acid (MES) (purity ≥ 99.5%), DL-Dithiothreitol (DTT) (purity ≥ 98%), and the sodium acetate trihydrate (purity ≥ 99.0%) were purchased from Sigma-Aldrich (Germany). Disodium hydrogen phosphate dehydrate (purity 99.5%) was purchased from Merck (Germany) and potassium dihydrogen phosphate (purity ≥ 98%) from AppliChem (Germany). L(+)-Ascorbic acid (purity 99.1%), sodium chloride (purity 99.9%), acetonitrile (purity 99.9%) and Ultrapure water came from VWR (Germany). Freeze-dried chicken pancreas was purchased from Pel-Freez Biologicals (USA), rat serum came from Biozol (Germany). The unlabeled reference compounds: folic acid; 10-formylfolic acid; (6R,S)-5-formyl-5,6,7,8-tetrahydrofolic acid, calcium salt (5-formyl-tetrahydrolfolate); (6R,S)-5-methyl-5,6,7,8-tetrahydrofolic acid, calcium salt (5-methyl-tetrahydrofolate); (6S)-5,6,7,8-tetrahydrofolic acid (tetrahydrofolate) were purchased from Schircks Laboratories (Switzerland). The internal standards [$^{13}C_5$]-folic acid, [$^{13}C_5$]-(6S)-tetrahydrofolate, [$^{13}C_5$]-(6S)-5methyl-tetrahydrofolate, calcium salt, [$^{13}C_5$]-(6S)-5-formyl-tetrahydrofolate and calcium salt were purchased from Schircks Laboratories (Switzerland). Phosphate buffer (PBS), bovine serum albumin (BSA), paraformaldehyde (PFA), and agarose were purchased from Euromedex (France). The monoclonal anti5-

110 methyltetrahydrofolic acid from mouse (first antibody) and Mowiol was purchased from Sigma-Aldrich
111 (France). The anti-mouse Alexa 488 from goat (second antibody) was purchased from Invitrogen (USA).

112 ***2.2 Soaking experiments***

113 Soaking was performed as described by Coffigniez et al., (2018). Different soaking conditions were
114 tested with a water-to-seed ratio of 4:1 (w/w) in a water bath. The following temperature-time values
115 were investigated: 30 °C /3 h-6 h-14 h, 60 °C/1 h-2 h-4 h and 95 °C/0.5 h-1 h-1.5 h-2 h. After being
116 processed, the seeds were freeze-dried and stored, like the soaking water, at – 80 °C for a maximum of
117 two weeks before folate quantification. For the localization of the folate, after soaking, the seeds were
118 immediately immerged in a 70% (v/v) ethanol solution. Each soaking experiment was performed in
119 duplicate.

120 ***2.3 Folate quantification***

121 Folate was quantified as described by Striegel et al., (2018).

122 ***2.3.1 Preparation of the solution***

123 MES buffer was made of 21.3 g of MES hydrate and 10.0 g of ascorbic acid in 500 mL of MilliQ
124 water, with the pH adjusted to 5.0. Phosphate buffer was made of 1.41 g of Na_2HPO_4 and 1.36 g of
125 KH_2PO_4 in 100 mL of MilliQ water, with the pH adjusted to 7.0. The elution buffer was made of 5.0 g of
126 NaCl, 1.36 g of sodium acetate trihydrate, 1.0 g of ascorbic acid and 0.1 g of DTT in 100 mL of MilliQ
127 water. The chicken pancreas was prepared by dissolving 30 mg and 0.3 g of ascorbic acid in 30 mL of
128 phosphate buffer with the pH adjusted to 7.0. Rat serum was used as obtained from Biozol.

129 ***2.3.2 Folate extraction***

130 The freeze-dried seeds were ground in a coffee grinder (Rommelsbacher, Germany). In some cases,
131 grinding was continued using a mortar. The folates were extracted from 100 mg of soaked-cooked
132 cowpea flour in 10 mL of MES buffer. To the samples, solutions of the internal standards were added in
133 amounts to fall within the given range of calibration. The samples were boiled for 10 min to facilitate
134 extraction and then cooled down on ice. To obtain complete deconjugation, 2 mL of chicken pancreas
135 suspension and 400 µL of rat serum were added and the samples were incubated overnight in a shaking
136 water bath at 37 °C. Next, the samples were boiled again for 10 min and cooled on ice to inactivate the
137 enzymes. Acetonitrile (10 mL) was added and the samples were centrifuged for 20 min at 4000 rpm and
138 4 °C. The supernatant was decanted. The extract was purified by solid phase extraction (SPE) on strong
139 anion exchange (SAX, quaternary amine, 500 mg, 3 mL) (Phenomenex, Germany) and finally
140 concentrated in 2 mL of elution buffer. The samples were filtered through a 0.22 µm membrane filter.

141 ***2.3.3 Folate quantification***

142 Folates were then separated by liquid chromatography coupled with tandem mass spectrometry (LC-
143 MS-MS). The separation was carried out on a Shimadzu Nexera X2 UHPLC system with a model DGU-
144 20ASR degassing unit (Shimadzu, Japan). The folates were separated at 30 °C on a 2.7 µm,
145 100 × 2.1 mm C18-LC column (Restek, Germany), coupled with a PDA Nexera SPD-M30A diode array
146 detector (Shimadzu, Japan). The ionization mode was positive electrospray. The injection volume was
147 10 µl. The mobile phases were a gradient constituted of 0.1% formic acid in water and 0.1% formic acid
148 in acetonitrile. The flow rate was 0.4 µL/min. Both extraction and measurements were done in duplicate
149 for each soaking experiment.

150 The concentration of unlabeled analytes was determined before each extraction. Quantification was
151 performed using a calibration curve with external standards. Separation was performed by High-
152 performance Liquid Chromatography (HPLC), coupled with a SPA-M20A diode array detector
153 (Schimadzu, Japan). The folates were separated at room temperature on a nucleosil 100-5 C18 EC, 250 x
154 3 mm column (Macherey-Nagel, Germany). The injection volume was 10 µl. The mobile phases were a
155 gradient comprising of 0.1% of acetic acid in water and methanol. The flow rate was 0.4 $\mu L.min^{-1}$.

156 ***2.4 Folate distribution in seeds by immunostaining***

157 After soaking, the seeds were immersed in 4% paraformaldehyde in PBS (phosphate buffer) (pH=7.0,
158 0.01M) for 48 h. The seeds were then rinsed for 15 min in a solution of PBS/Glycin 0.1 M and two times
159 for 15 min in PBS. The cotyledon and embryonic axis of the seeds (Figure 1) were separated using a
160 razor blade. The embryonic axis was embedded in 5% agarose and cut using a vibratome (Microm,
161 France) while the cotyledon was directly cut using a vibratome. The thicknesses of the resulting cross
162 sections samples were 50 µm and 30 µm for cotyledon and embryonic axis respectively. The sliced
163 tissues then were immersed for 2 h in a blocking solution composed of 5% BSA in PBS. The first
164 antibody: 5-methyltetrahydrofolic acid, was diluted 1/500 in blocking solution and left on the samples for
165 one night at 4 °C with agitation. The samples were then rinsed three times for 10 min in a solution of
166 PBS at room temperature. Next, the samples were immersed in the second antibody: Alexa 488 2 mg/ml
167 (Invitrogen, France) diluted 1/500 in blocking solution, then rinsed three times for 10 min in a solution of
168 PBS at room temperature. The cross sections were collected on microscopic slides with Mowiol. Each
169 immunostaining experiment was performed in duplicate. The microscopic analyses were performed using
170 a Droit Zeiss 880 Laser Coherent Chameleon Ultra II Multiphoton microscope and a confocal Zeiss
171 LSM880 Airyscan microscope. The excitation wavelength was 488 nm and the emission wavelength was
172 523 nm.

173 **3. Multi-response modeling**

174 ***3.1 Assumptions***

175 Cowpea seed is assumed to be pseudo-ellipsoidal with a 2D-symmetric axis (Γ_2 boundary) as
176 described by Coffigniez et al., (2018) (fig. 1). Two domains are considered here: the single cowpea seed
177 (Ω_S) and the soaking water medium (Ω_{SW}). These two domains are separated by an interface (Γ_1).
178 While the cowpea is soaking, folate vitamers are interconverted or metabolized within the cowpea seeds
179 but also diffused out of it. Folic acid, 5-formyl-tetrahydrofolate and 10-formylfolic acid can be
180 enzymatically or chemically converted into 5-methyl-tetrahydrofolate. The 5-methyl-tetrahydrofolate can
181 be thermally degraded into pyrazino-s-triazin by oxidation.

182 Concerning the model, the following assumptions were formulated:

183 (A1) Folate vitamer concentrations are homogeneous in the seeds, and the seed matrix is also considered
184 to be homogeneous and non-porous, with folate already being in soluble form in cytosol.

185 (A2) The soaking water is considered as perfectly stirred, with no solute gradients.

186 (A3) The seed volume remains constant during soaking (no swelling).

187 (A4) Except for folates, no dry matter is lost into the soaking water during soaking.

188 (A5) The concentration of tetrahydrofolate is negligible.

189 (A6) Fick's laws of diffusion describe the transport of folates.

190 (A7) The folate interconversion, metabolization and oxidation follow first-order kinetics in the seeds and
191 are not considered in the soaking water.

192 The eight state variables considered in our study were the concentrations (kg m^{-3}) both in seed
193 ($\Omega_i = \Omega_S$) and soaking water ($\Omega_i = \Omega_{SW}$) of folic acid (PteGlu) (C_1), 10-formylfolic acid (C_2),
194 5-formyl-H_4folate (C_3) and 5-methyl-H_4folate (C_4) concentrations. Concentrations are also expressed in
195 µg/100g (db).

196 ***3.2. The unsteady-state diffusion-reaction model***

197 The mass-balance equations for folates in cowpea seeds (Ω_S, Eq. (1)) and soaking water
198 (Ω_{SW}, Eq. (2)) can be written as:

$$\left.\begin{aligned}
&\frac{\partial C_{1,\Omega_S}}{\partial t}-\nabla\left(D_1\nabla C_{1,\Omega_S}\right)=-k_{1,\Omega_S}C_{1,\Omega_S}\\
&\frac{\partial C_{2,\Omega_S}}{\partial t}-\nabla\left(D_2\nabla C_{2,\Omega_S}\right)=-k_{2,\Omega_S}C_{2,\Omega_S}\\
&\frac{\partial C_{3,\Omega_S}}{\partial t}-\nabla\left(D_3\nabla C_{3,\Omega_S}\right)=-k_{3,\Omega_S}C_{3,\Omega_S}\\
&\frac{\partial C_{4,\Omega_S}}{\partial t}-\nabla\left(D_4\nabla C_{4,\Omega_S}\right)=-k_{4,\Omega_S}C_{4,\Omega_S}+k_{1,\Omega_S}C_{1,\Omega_S}+k_{2,\Omega_S}C_{2,\Omega_S}+k_{3,\Omega_S}C_{3,\Omega_S}
\end{aligned}\right\} \quad (1)$$

$$V_{\Omega_{SW}}\frac{\partial C_{i,\Omega_{SW}}}{\partial t}=J_X \quad (2)$$

With $C_{i,\Omega_{SW}}$ (eq.(2)) being the concentration of any considered folate species in soaking water and D_i (i = 1,…4) are the apparent diffusivities ($m^2.s^{-1}$) of PteGlu, 10-CHO-PteGlu, 5-CHO-H_4folate and 5-CH_3-H_4folate respectively. The overall reaction scheme is displayed in figure 2.

Equations (1), and (2) have the following initial and boundary conditions:

$$C_{i,\Omega_S}=C_{i,\Omega_S,0} \quad \text{in } \Omega_S \text{ for } t=0 \quad (3)$$

$$C_{i,\Omega_{SW}}=0 \quad \text{in } \Omega_{SW} \text{ for } t=0 \quad (4)$$

$$C_{i,\Omega_S}=C_{i,\Omega_{SW}} \quad \text{on } \Gamma_1 \quad (5)$$

$$\nabla C_{i,\Omega_S}\cdot\vec{n}=0 \quad \text{on } \Gamma_2$$

(6)

where $C_{i,\Omega_S,0}$ are the initial content ($kg.m^{-3}$) of component i in Ω_S.The outgoing mass flux J_i ($kg\ s^{-1}$) of folate i through the cowpea seed/soaking water interface (Γ_1) is expressed as:

$$J_i=-AD_i\nabla C_{i,\Omega_S} \quad (7)$$

where A is the surface area of the seed in contact with the soaking water (m^2), and C_{i,Ω_i} are the concentrations of component X ($kg.m^{-3}$). Model input parameters are listed in table 1. As already performed on alpha-galactosides by Coffigniez et al. (2018), a mass balance analysis of the diffusion-

reaction processes inside the seed was performed. The produced fractions of folates *i* induced by reaction ($m_{i,prod}$), the degraded fractions induced by reaction ($m_{i,degr}$), the transferred fractions induced by diffusion ($m_{i,diff}$) and the residual fraction ($m_{i,res}$) expressed in relation to the initial mass ($m_{i,0}$), were obtained by solving the following integral equations:

$$\frac{m_{i,prod}}{m_{i,0}} = \int_t \left(\iint_{\Omega_S} k_{i,\Omega_S} C_{i,\Omega_S} dV_{\Omega_S} \right) dt \tag{8}$$

$$\frac{m_{i,degr}}{m_{i,0}} = \int_t \left(\iint_{\Omega_S} -k_{i,\Omega_S} C_{i,\Omega_S} dV_{\Omega_S} \right) dt \tag{9}$$

$$\frac{m_{i,diff}}{m_{i,0}} = \int_t J_i \, dt \tag{10}$$

$$\frac{m_{i,res}}{m_{i,0}} = \frac{m_{i,0} + m_{i,prod} - m_{i,diff} - m_{i,\deg}}{m_{i,0}} \tag{11}$$

3.3. Numerical solution

The numerical solution was obtained in the same way as described by Coffigniez et al., (2018), with the initial conditions given by Eqs. (3) and (4), and the boundary conditions given by Eqs. (5) and (6) using the FEM-based commercial Comsol Multiphysics™ (version 5.2a, Comsol Inc., Stockholm, Sweden). A 5 000-element mesh was created in Comsol. The linearized problem was solved by the MUMPS time-dependent solver (Multifrontal Massively Parallel Solver) which implements a parallel distributed LU factorization of large sparse matrixes. The maximum time step was 0.05 s and the Jacobian was updated at each iteration. The typical simulation time was five minutes using a 3.25 Gb free memory (RAM) and 3-GHz Intel core Duo CPU computer (32 bits).

3.4. Parameter identification

Both apparent diffusivities (D_i) and rate constants ($k_{i,\Omega}$) were identified using the method described by Coffigniez et al., (2018). In this multi-response modeling approach, the model parameters were iteratively adjusted to the goodness-of-merit (determinant of dispersion matrix between experimental and predicted data) using a minimization procedure of the Nelder-Mead simplex with the "fminsearch"

238 function of Matlab software. The standard deviation of each adjusted parameter was determined by
239 Monte Carlo simulations with 200 draws.

240 **4. Results and discussion**

241 ***4.1. Folate concentration in raw seeds***

242 Table 2 shows the initial concentrations of folic acid (PteGlu, $C_{1,0}$), 10-formylfolic acid (10-
243 CHO- PteGlu, $C_{2,0}$), 5-formyltetrahydrofolate (5-CHO-H_4folate, $C_{3,0}$), 5-methyltetrahydrofolate (5-CH_3-
244 H_4folate, $C_{4,0}$) and tetrahydrofolate (H_4folate) in raw cowpea seeds and more specifically in cotyledons
245 and in the embryonic axis. In raw seeds, 5-CHO-H_4folate represented 54% of the total folate content. The
246 latter vitamer is probably the storage form of folates and is more stable than the active form 5-CH_3-
247 H_4folate (Saini et al., 2016). 5-CH_3-H_4folate, PteGlu and 10-CHO- PteGlu represented 12%, 16% and
248 16% of the total folate content, respectively, and the H_4folate concentration was negligible. Strandler et
249 al., (2015) also showed that the formyl forms were the most abundant forms in chickpea (49%).
250 However, other studies reported that the majority form was 5-CH_3-H_4folate or H_4folate in legumes (in
251 pea, mung bean, lentil, cowpea and soybean) (Rychlik et al., 2007; Delchier et al., 2016). For example, 5-
252 CH_3-H_4folate was reported to represent 75% of total folate in pea (Ringling and Rychlik, 2012).

253 As can be seen in table 2 all vitamers were more concentrated in the embryonic axis than in the
254 cotyledons. For example, the concentrations of 5-CH_3-H_4folate and 5-CHO-H_4folate were two to three
255 times higher in the embryonic axis than in the cotyledon. However, the embryonic axis represented only
256 2.3% of the total seed mass, which explains why the concentration in raw seeds was similar to the
257 concentration in cotyledons (around 400 µg/100 g db). These observations were confirmed by
258 immunostaining of 5-methyltetrahydrofolate in cowpea seeds (figure 3). Indeed, a relatively larger
259 quantity (i.e. fluorescence signal here) of folates was observed in the embryonic axis (root meristem) (fig.
260 3a) than in the cotyledons (fig. 3b), which seems to be consistent with the results of quantification
261 (table 4). These results are also comparable with results in the literature. For instance, Hoppner and
262 Lampi, (1993) reported a concentration of 367.1 ± 28.6 µg/100 g db in cowpea seeds, and Gambonnet et
263 al., (2001) also reported that the concentration of folates in pea was 5 to 10 times higher in the embryonic
264 axis than in cotyledons. However, the embryonic axis accounts for only 2% of the seeds, so the majority
265 of folate was located in the cotyledons (Gambonnet et al., 2001). Folates synthesis is high in the root
266 meristem because folate is largely consumed in the dividing cells to synthesize thymidylate and purine
267 (Rébeillé et al., 2006; Gorelova et al., 2017). In cells, H_4folate and 5-CHO-H_4folate are mostly present in
268 mitochondria, whereas 5-CH_3-H_4folate is most abundant in cytosol (Gorelova et al., 2017). Folates have
269 also been reported to be present in vacuoles and chloroplasts (Rébeillé et al., 2006). However, the
270 H_4folate concentration in raw seed was observed to be lower than described by others authors (Gorelova

et al., 2017) and the PteGlu concentration was found to be higher than described by others authors. This might be due to H4folate oxidization into PteGlu during sample transport and/or storage.

4.2. Folate kinetics during soaking

4.2.1. Experimental changes in folates contents during soaking

Figure 4 shows the folate content kinetics both in the seeds and soaking water at 95 °C. After 2 h, the concentrations of PteGlu, 10-CHO- PteGlu, 5-CHO-H_4folate and 5-CH_3-H_4folate were reduced by 33%; 54%; 53% and 69%, respectively, in seeds representing a 50% loss of total folates. The respective fractions of 10-CHO-PteGlu and 5-CHO-H_4folate were entirely transferred to the soaking water with constant net contents (i.e. sum in the seeds and in the soaking water). However, the net content of 5-CH_3-H_4folate was 21% lower than the initial amount in raw seeds. The decrease in this vitamer was probably due to thermal oxidation. Indeed, the chromatograms revealed the appearance of pyrazino-s-triazin (also called MeFox; not quantified), the oxidation product of 5-CH_3-H_4folate in both seeds and soaking water. The net content of PteGlu was 22% higher after soaking at 95 °C for 2 h than in raw seeds. This can be explained by the fact that PteGlu can be produced by oxidation of H_4folate. These results are consistent with those reported in the literature. Hefni and Witthöft, (2014) reported a 32% reduction in folate in faba bean after boiling for 30 min using a water-to-seed ratio of 5:1 (w/w). About 90% of this loss was due to diffusion into the soaking water. Hoppner and Lampi, (1993) also reported an average 28% reduction in total folates after a short period (1 h) of soaking at room temperature followed by boiling for 90 min in different legume seeds steeped with a water-to-seed ratio of 3:1 (w/w). Similarly, Dang et al., (2000) found a of 53% reduction in total folates in chickpea and a 46% reduction pea, after soaking for 16 h at room temperature followed by boiling for 2 h in a water to seed ratio of 3:1 (w/w).

After soaking at 60 °C for 4 h (Figure 5), the PteGlu, 10-CHO-PteGlu, 5-CHO-H_4folate and 5-CH_3-H_4folate concentrations were reduced in seeds by 63%, 60%, 50% and 39%, respectively. The loss of 10-CHO-PteGlu and 5-CHO-H_4folate in the seeds were fully explained by mass transfer into the soaking water. However, the net content of PteGlu was 33% lower than its initial content, and the net content of 5-CH_3-H_4folate was 41% higher than its initial concentration. We thus assumed that this was due to the chemical conversion of PteGlu into 5-CH_3-H_4folate, as proposed in the reaction scheme in figure 2.

After soaking at 30 °C for 14 h (Figure 6), the PteGlu, 10-CHO-PteGlu, and 5-CHO-H_4folate concentrations in the seeds were reduced by 54%, 54%, and 82%, respectively, whereas the 5-CH_3-H_4folate concentration increased by 344%. The fraction transferred into the soaking water was only 25% for 10-CHO-PteGlu, and even less (5%) for the other vitamers. This marked reduction in PteGlu, 10-CHO-PteGlu and 5-CHO-H_4folate can be explained by the conversion of all these vitamers

304 into the active form (5-CH_3-H_4folate) as proposed in the reaction scheme (figure 2). This conversion
305 usually occurs when the seed physiologically prepare to germinate. Indeed, after the soaking process
306 (14 h), the net total folate concentration decreased only by 13% in seeds, which is in the same order of
307 magnitude as the folate losses (12%) found by Hoppner and Lampi, (1993) in cowpea and in the same
308 soaking conditions. The remaining folate content can be used for the development of the seed.
309 Nevertheless, the behavior of folate during soaking also depends to a great extent on the legume species
310 considered. For instance, Xue et al., (2011) reported a 31% reduction in 5-CH_3-H_4folate in navy bean
311 after soaking at room temperature for 12 h with a water-to-seed ratio of 3:1 (w/w), whereas Hefni and
312 Witthöft, (2014) found a 50% increase in folate content in faba beans in the same soaking conditions.
313 These differences could be due to the germination capacity of the seeds under given conditions.

314 ***4.2.2. Transport properties of folates***

315 Table 3 shows the adjusted apparent diffusivity of folates ($m^2.s^{-1}$) in cowpea seeds with the three
316 different soaking temperatures (30 °C, 60 °C and 95 °C). The model fitted the experimental data
317 satisfactorily with a mean RMSE of 10% (db). The different vitamers have a similar molar mass
318 (between 441 $g.mol^{-1}$ and 473 $g.mol^{-1}$). As a consequence, we expected the same order of magnitude for
319 the apparent diffusivity of all the vitamers at each temperature. However, apparent diffusivity was
320 significantly higher for 10-CHO-PteGlu than for the other forms. This difference could be explained by
321 the fact that the folates were not similarly distributed in the seeds and the distribution could vary
322 depending on the vitamer considered (Gorelova et al., 2017).

323 Apparent diffusivity increased with temperature for all the vitamers. For example, the adjusted
324 apparent diffusivity of 5-CHO-H_4folate was 1.5 fold higher at 95 °C than at 60 °C, and 82 fold higher at
325 60 °C than at 30 °C. Folate diffusion also depends on both food matrix structure and composition.
326 Although the literature on folate transport properties is quite poor, for the sake of comparison, Delchier et
327 al., (2014) obtained almost constant folate apparent diffusivity of $7.4 \pm 2.1 \times 10^{-12}$ m^2 s^{-1} in the case of
328 green beans soaked in the 25 °C to 65 °C temperature range. In the case of soaked cowpea, adjusted
329 folate apparent diffusivity was of the same order of magnitude as that found for alpha-galactosides in the
330 same cowpea cultivar (Coffigniez et al., 2018). For instance, for stachyose, apparent diffusivity of
331 0.02×10^{-11} $m^2.s^{-1}$, 3.0×10^{-11} $m^2.s^{-1}$ and 4.3×10^{-11} $m^2.s^{-1}$ respectively, were identified at 30 °C, 60 °C
332 and 95 °C. This marked increase in molecular diffusion with temperature can be linked with dramatic
333 changes in seed structure that take place during soaking. Indeed, the cell wall may be degraded and
334 solubilized by β-elimination during heating (Waldron et al., 2003). Cell walls and teguments probably
335 rupture between 30 °C and 60 °C, thus facilitating folate diffusion. This underlying structural mechanism
336 was confirmed by the immunostaining of 5-CH_3-H_4folate in cowpea seeds after different soaking
337 treatments. As shown in figure 7, raw seeds (pictures (a) and (b)) had concentrated folates inside the

338 cells. In contrast, immunostaining of 5-CH_3-H_4folate in the meristem roots of seeds soaked at 95 °C
339 showed folate diffusing into the intercellular spaces (pictures (e) to (h)). The shape of cells was lost,
340 which confirmed the possibility of pectin degradation that facilitated folate diffusion. At 60 °C, one part
341 of folate was still inside the cells while another part had already diffused outside the cell. The cell walls
342 probably started breaking down.

343 Image analysis of the pictures shown in figure 7 allowed us to estimate the relative concentration (%)
344 in 5-CH_3-H_4folate from the surface covered (dots) by the fluorescence signal. The concentration
345 calculated using this method was lower than absolute 5-CH_3-H_4folate quantification (Table 4). This could
346 be due to the fact part of the folate had diffused outside the embryonic axis, but had not yet left the seed.
347 The 5-CH_3-H_4folate immunostain biomarker showed no cross reactivity with folic acid, but cross
348 reactivity with 5-CHO-H_4folate is nevertheless conceivable. However, the larger difference in the results
349 of image quantification and 5-CHO-H_4folate quantification led us think that there was no cross reactivity
350 with 5-CHO-H_4folate in this case.

351 ***4.2.3 Thermal degradation and conversion of folates***

352 Thermal degradation rates (k, s^{-1}) were adjusted to experimental data assuming first order kinetics
353 (table 3). Results showed that thermal degradation increased with temperature. Thermal degradation was
354 clearly visible in the case of 5-CH_3-H_4folate at 95 °C as described above (figure 4). Its increasing
355 intensity in the respective MRM transition indicated that pyrazino-s-triazin was generated by oxidation of
356 5-CH_3-H_4folate (Ringling and Rychlik, 2017). In the literature, 5-CH_3-H_4folate oxidation has already
357 been reported and modeled (assuming fist-order kinetics) but only in the case of standard solutions (Oey
358 et al., 2006; Verlinde et al., 2010; Munyaka et al., 2010). For example, Oey et al., (2006) estimated the
359 thermal degradation rate of 5-CH_3-H_4folate to be in the range [7.8×10^{-6}–4.3×10^{-4} s^{-1}] for temperatures
360 ranging from 25 °C to 80 °C. These results are in agreement with those of Viberg et al., (1997). However,
361 the latter authors showed that the thermal degradation rate decreased with increasing initial folate
362 concentration and decreasing oxygen concentration. Our model was simplified by assuming that the
363 whole oxidation process only takes place in the seeds and not in the soaking water. Due to the high
364 diffusion of 5-CH_3-H_4folate at high temperature (60 °C and 95 °C), the oxidation of 5-CH_3-H_4folate
365 could also occur in the soaking water. However, it was not possible for us to distinguish between the
366 oxidation contributions from the two compartments.

367 The increase in PteGlu concentration after soaking at 95 °C could be explained by oxidation of
368 H_4folate ($k = 2.42 \pm 0.04\times10^{-4}s^{-1}$, data not shown) as already reported in the literature (Strandler et al.,
369 2015). Due to the low concentration in H_4folate and the low rate of thermal degradation of folates at both
370 30 °C and 60 °C (decrease in H_4folate less than 5 µg/100g bs), the production of PteGlu at 60 °C and

371 30 °C was consequently negligible. PteGlu, 10-CHO-PteGlu and 5-CHO-H_4folate were found to be stable
372 at 95 °C with no thermal degradation. At lower soaking temperatures (30 °C), the reduction of PteGlu,
373 10-CHO-PteGlu and 5-CHO-H_4folate was due to enzymatic conversion into 5-CH_3-H_4folate. The
374 conversion rate constant (*k*) was adjusted to experimental data (table 3). All conversions mainly occurred
375 at 30 °C in seeds and can therefore be attributed to enzyme action. The enzymatic conversion was
376 assumed to be negligible in the soaking water because the diffusion of enzymes from the seed to soaking
377 water was assumed to be negligible due to their high molar mass (section 4.2.2). The enzymatic
378 conversion within the seed was 2.7 times higher for PteGlu than for 10-CHO-PteGlu and 3.6 times higher
379 for 5-CHO-H_4folate than for PteGlu. These interconversions are shown in the folate reaction scheme in
380 figure 2. This scheme was simplified for the purpose of modeling. Indeed, we assumed that PteGlu, 10-
381 CHO-PteGlu and 5-CHO-H_4folate were converted into 5-CH_3-H_4folate without taking any intermediary
382 products in account. In the literature, with the exception of 10-CHO-PteGlu, interconversions of the
383 different folate vitamers have already been reported. PteGlu can be reduced into H_4folate by
384 dihydrofolate reductase (Jägerstad and Jastrebova, 2013). Then, H_4folate can be converted into 5-CH_3-
385 H_4folate by serinehydroxymethyltransferase and 5,10-methylenetetrahydrofolate reductase (Rébeillé et
386 al., 2006). H_4folate can also be converted into 5-CH_3-H_4folate via intermediate 10-CHO-H_4folate by 10-
387 formyltetrahydrofolate synthase (Rébeillé et al., 2006) followed by 10-CHO-H_4folate conversion into 5-
388 CH_3-H_4folate by 5,10-methylenetetrahydrofolate dehydrogenase and 5,10-methylenetetrahydrofolate
389 reductase (Rébeillé et al., 2006; Jägerstad and Jastrebova, 2013). Finally, 5-CHO-H_4folate can be
390 converted into 5-CH_3-H_4folate by 5,10-methenyltetrahydrofolate synthetase, 5,10-methylene-
391 tetrahydrofolate dehydrogenase and 5,10-methylenetetrahydrofolate reductase (Jägerstad and Jastrebova,
392 2013). Moreover, 10-CHO-H_4folate can also be chemically converted into 5-CHO-H_4folate besides
393 being the direct precursor for 10-CHO-PteGlu formed by oxidation (Jägerstad and Jastrebova, 2013).
394 Therefore, 5-CHO-H_4folate may also be an intermediate in the interconversion of PteGlu.

395 The enzymatic reactions are usually modeled using the Michaelis-Menten equation. However, in the
396 case of folates, the overall enzymatic conversion scheme is complex since it involves too many enzymes
397 and substrates that would each need to be quantified. That is why we modeled the enzymatic conversions
398 assuming first order kinetics that are equivalent to a Michaelis-Menten approach if the concentration of
399 substrate is low compared to the Michaelis consant K_m.

400 The decrease in total folate concentration at 30 °C can be explained by the oxidation of 5-CH_3-
401 H_4folate (generation of pyrazino-s-triazin, see section 4.2.4). However, under these conditions, this
402 decrease could also be partly due to the metabolic activity of the seeds, i.e. the integration of the formyl
403 group into DNA and the use of 5-CH_3-H_4folate in methylation reactions and in the methionine synthesis
404 (Scott et al., 2000; Gorelova et al., 2017).

405 At 60 °C, it can be assumed that the enzymes were partly thermally degraded and hence that the
406 enzymatic interconversion did not occur. Consequently, only the chemical interconversion of PteGlu into
407 5-CH_3-H_4folate, hypothesized from our experiments (figure 5), was modeled. The net concentration of
408 10-CHO-PteGlu (sum of the concentration in the seeds and that in the soaking water) was quite low after
409 soaking at 60 °C for 4 h (loss of 7 µg/100g), but this loss was disregarded in the model.
410 5-CHO-H_4folate remained constant during the soaking process at 60 °C and, therefore, the
411 interconversion of 5-CHO-H_4folate was disregarded. However, like at 30 °C, it is possible that 5-CHO-
412 H_4folate was an intermediate or by-product of 5-CH_3-H_4folate production.

413 ***4.3 Folates: reaction vs. diffusion during soaking***

414 Figure 8 shows changes in the predicted diffused, degraded (oxidation or interconversion), produced
415 (enzymatic) and the residual folate fractions in cowpea seeds during soaking at different temperatures. At
416 both 95 °C and 60 °C, the diffused fraction predominated, whereas at 30 °C, the degraded and produced
417 fractions were predominant, especially 5-CHO-H_4folate and 5-CH_3-H_4folate. After soaking at 95 °C for
418 2 h, the diffused fraction of folate vitamers represented between 43.7% (5-CH_3-H_4folate) and 65.9% (10-
419 CHO-PteGlu) of their initial concentrations. Only a degraded fraction of 5-CH_3-H_4folate was detected
420 that represented 27.6% (oxidation to pyrazino-s-triazin). Only the production of PteGlu was significant
421 and represented 19.4 % (oxidation of H_4folate). After soaking at 60 °C for 4 h, the diffused fraction also
422 predominated for all vitamers with a proportion ranging between 32.2% (PteGlu) and 69.6% (5-CH_3-
423 H_4folate). The degraded fraction represented around 29% for PteGlu (interconversion into 5-CH_3-
424 H_4folate) and 5-CH_3-H_4folate (oxidation to pyrazino-s-triazin). Production was only detectable of 5-CH_3-
425 H_4folate and represented 40.3% (interconversion of PteGlu). In the two latter, the produced and degraded
426 fractions resulted in an even total folate balance. Soaking at 95 °C for 2 h or at 60 °C for 4 h led to the
427 diffusion of 50% of total folate into the soaking water.

428 For all vitamers and after soaking at 30 °C for 14 h, the diffused fraction was much lower than after
429 soaking at 60 °C and 95 °C. This difference was due to the high production of 5-CH_3-H_4folate (by folate
430 interconversions) at 30 °C and the high diffusion coefficient in the case of 10-CHO-PteGlu at higher
431 temperatures. Indeed, after soaking for 14 h, the produced fraction of 5-CH_3-H_4folate was about 572.8%
432 while in parallel the degraded fraction represented 65.8%, 31.7% and 93.3% of PteGlu, 10-CHO-PteGlu
433 and 5-CHO-H_4folate, respectively. This high percentage of 5-CH_3-H_4folate production was because the
434 initial quantity of 5-CHO-H_4folate in the seeds was higher than that of 5-CH_3-H_4folate. As a result, the
435 final net concentration in seeds (i.e. the residual fraction) of 5-CHO-H_4folate decreased to 2.8% of the
436 initial concentration after soaking at 30 °C for 14 h and the 5-CH_3-H_4folate concentration increased to
437 429.8%. During this process, oxidation or the use of 5-CH_3-H_4folate in methylation reactions resulted in a
438 degraded fraction representing 218.4%.

439 In this model, two phenomena were simultaneously taken into account, (*i*) mass transport and (*ii*)
440 first-order reactions that both affected the concentrations of folates in the seeds. In any case, the mutual
441 correlation coefficient between the different model parameters (Eq. (1)) was lower than 0.21, confirming
442 that minimizing the determinant of dispersion matrix between experiments and predicted concentrations
443 is a reliable method to identify the parameters, as recommended by Van Boekel, Martinus A.J.S, (2008).
444 A sensitivity study has been performed and showed that a variation of ± 15% of any model
445 parameter induced a mean overall deviation of about 22% compared to the model adjustment that
446 provides the best fitting performance (minimal RMSE).

447 ***4.4 Soaking recommendations***

448 In West Africa, cowpea seeds are usually prepared using two different methods. The first consists in
449 directly boiling the seeds in water for 1 h (Madodé, 2012), and the second involves a pre-soaking step at
450 room temperature (about 30 °C) for one night followed by boiling in water for 25 min (Madodé, 2012).
451 After soaking at 95 °C for 1 h (figure 8) the model showed a residual concentration of total folates of
452 62% (260 µg/100g bs), whereas an 8 h pre-soaking step (residual concentration of 77%) followed by
453 boiling for 25 min (residual concentration of 74%) resulted in a residual concentration of total folate of
454 57% (242 µg/100g bs). Therefore, these two different methods resulted in a similar decrease in total
455 folate concentration. However, this is not the case if each vitamer is considered separately. Indeed, after
456 direct boiling (first method), the 260 µg/100g of total folate were composed of 59.1% of 5-CHO-
457 H_4folate, 19.7% of PteGlu, 12.9% of 10-CHO-PteGlu and 8.3% of 5-CH_3-H_4folate. After soaking
458 combined with boiling (second method), the 242 µg/100g of total folate consisted of 67.5% of 5-CH_3-
459 H_4folate, 12.1% of PteGlu, 11.2% of 5-CHO-H_4folate and 9.2% of 5-CHO-H_4folate. Of all the vitamers
460 present in seeds, 5-CH_3-H_4folate is considered to be the most bioavailable (Striegel et al., 2018).
461 Therefore, a pre-soaking step at 30 °C leads to interconversion of folates into this vitamer and, hence,
462 increases folate bioavailability.

463 The daily recommendations for folate intake are 120-300 µg for children and 300 µg for adults
464 (Krawinkel et al., 2014). Therefore, 100 g bs of cowpea, which corresponded to 160 g after soaking-
465 cooking (Coffigniez et al., 2018) would be sufficient in terms of FDE to fulfil the daily requirements of
466 both children and adults.

467 **5. Conclusion**

468 Our study advanced our knowledge on the contrasted behavior of folate vitamers in cowpea seeds as
469 a function of the soaking conditions. The folates were mainly composed of 5-CHO-H_4folate (storage
470 form) and were more concentrated in the embryonic axis than in the cotyledons. For the first time, a 2D

axi-symmetric model was built, considering a single cowpea seed being soaked in soaking water and taking into account the diffusion, conversion, and oxidation of folates. The model fitted the data satisfactorily and the results showed the predominant transport of folate out of the seeds after a soaking process at 60 °C or 95 °C. Immunostaining experiments on cowpea seed cross sections underlined these phenomena. At lower temperature (30 °C), PteGlu, 10-CHO-PteGlu and 5-CHO-H_4folate were mainly interconverted into 5-CH_3-H_4folate (active form) while diffusion of all vitamers was very slow. At all temperatures, 5-CH_3-H_4folate was oxidized into pyrazino-s-triazin. The model was then used to predict losses due to diffusion and degradation during soaking-cooking process. The two traditionally used soaking-cooking methods in West Africa resulted in a similar loss of folates in seeds. Concerning folate bioavailability for human consumption, a pre-soaking step is recommended to promote enzymatic conversion into 5-CH_3-H_4folate. To advance further, germination could be tested for even better folate preservation and production.

Acknowledgements

This study was conducted in the framework of the ICOWPEA project funded under the "Thought for Food" Initiative by *Agropolis Fondation*, Fondazione Cariplo and Daniel et Nina Carasso Fondation under the reference ID 1507-031 through the "*Programme Investissements d'Avenir*" (Grant number: ANR-10-LABX-0001-01) and the VITAMICOWPEA project funded by ANR (French National Research Agency) by the *Agropolis Fondation* under the reference ID 1502-501, through the "*Programme Investissements d'Avenir*" (Labex Agro: ANR-10-LABX-0001-01).
Also, we want to thank COST Action CA15118 for their complementary financial PhD international mobility support.

References

Arcot, J., Shrestha, A., 2005. Folate: methods of analysis. Trends in Food Science & Technology 16, 253–266.

Coffigniez, F., Briffaz, A., Mestres, C., Alter, P., Durand, N., Bohuon, P., 2018. Multi-response modeling of reaction-diffusion to explain alpha-galactoside behavior during the soaking-cooking process in cowpea. Food chemistry 242, 279–287.

Crews, T.E., Peoples, M.B., 2004. Legume versus fertilizer sources of nitrogen: ecological tradeoffs and human needs. Agriculture, Ecosystems & Environment 102, 279–297.

Dang, J., Arcot, J., Shrestha, A., 2000. Folate retention in selected processed legumes. Food Chemistry 68, 295–298.

De Boer, J., Aiking, H., 2011. On the merits of plant-based proteins for global food security: Marrying macro and micro perspectives. Ecological Economics 70, 1259–1265.

504 Delchier, N., Herbig, A.-L., Rychlik, M., Renard, C.M., 2016. Folates in fruits and vegetables: Contents,
505 processing, and stability. Comprehensive Reviews in Food Science and Food Safety 15, 506–528.
506 Delchier, N., Ringling, C., Maingonnat, J.-F., Rychlik, M., Renard, C.M.G.C., 2014. Mechanisms of
507 folate losses during processing: Diffusion vs. heat degradation. Food Chemistry 157, 439–447.
508 https://doi.org/10.1016/j.foodchem.2014.02.054
509 El-Adawy, T.A., 2002. Nutritional composition and antinutritional factors of chickpeas (Cicer arietinum
510 L.) undergoing different cooking methods and germination. Plant Foods for Human Nutrition 57,
511 83–97.
512 Gambonnet, B., Jabrin, S., Ravanel, S., Karan, M., Douce, R., Rébeillé, F., 2001. Folate distribution
513 during higher plant development. J. Sci. Food Agric. 81, 835–841.
514 https://doi.org/10.1002/jsfa.870
515 Gonçalves, A., Goufo, P., Barros, A., Domínguez-Perles, R., Trindade, H., Rosa, E.A., Ferreira, L.,
516 Rodrigues, M., 2016. Cowpea (Vigna unguiculata L. Walp), a renewed multipurpose crop for a
517 more sustainable agri-food system: nutritional advantages and constraints. Journal of the Science
518 of Food and Agriculture 96, 2941–2951.
519 Gorelova, V., Ambach, L., Rébeillé, F., Stove, C., Van Der Straeten, D., 2017. Folates in Plants:
520 Research Advances and Progress in Crop Biofortification. Frontiers in Chemistry 5.
521 Graham, P.H., Vance, C.P., 2003. Legumes: importance and constraints to greater use. Plant physiology
522 131, 872–877.
523 Hefni, M., Witthöft, C.M., 2014. Folate content in processed legume foods commonly consumed in
524 Egypt. LWT-Food Science and Technology 57, 337–343.
525 Hoppner, K., Lampi, B., 1993. Folate retention in dried legumes after different methods of meal
526 preparation. Food Research International 26, 45–48.
527 Iqbal, A., Khalil, I.A., Ateeq, N., Khan, M.S., 2006. Nutritional quality of important food legumes. Food
528 Chemistry 97, 331–335.
529 Jägerstad, M., Jastrebova, J., 2013. Occurrence, stability, and determination of formyl folates in foods.
530 Journal of agricultural and food chemistry 61, 9758–9768.
531 Krawinkel, M.B., Strohm, D., Weissenborn, A., Watzl, B., Eichholzer, M., Bärlocher, K., Elmadfa, I.,
532 Leschik-Bonnet, E., Heseker, H., 2014. Revised DA-CH intake recommendations for folate: how
533 much is needed? European journal of clinical nutrition 68, 719.
534 Madodé, Y.E., 2012. Keeping local foods on the menu: a study on the small-scale processing of cowpea,
535 GVO drukkers & vormgevers B.V., Ponsen & Looijen. ed. The Netherlands.
536 Munyaka, A.W., Verlinde, P., Mukisa, I.M., Oey, I., Van Loey, A., Hendrickx, M., 2010. Influence of
537 Thermal Processing on Hydrolysis and Stability of Folate Poly-γ-glutamates in Broccoli (Brassica

oleracea var. italica), Carrot (Daucus carota) and Tomato (Lycopersicon esculentum). Journal of agricultural and food chemistry 58, 4230–4240.

Oey, I., Verlinde, P., Hendrickx, M., Van Loey, A., 2006. Temperature and pressure stability of L-ascorbic acid and/or [6s] 5-methyltetrahydrofolic acid: A kinetic study. European Food Research and Technology 223, 71–77.

Rébeillé, F., Ravanel, S., Jabrin, S., Douce, R., Storozhenko, S., Van Der Straeten, D., 2006. Folates in plants: biosynthesis, distribution, and enhancement. Physiologia Plantarum 126, 330–342.

Ringling, C., Rychlik, M., 2017. Simulation of food folate digestion and bioavailability of an oxidation product of 5-methyltetrahydrofolate. Nutrients 9, 969.

Ringling, C., Rychlik, M., 2012. Analysis of seven folates in food by LC–MS/MS to improve accuracy of total folate data. European Food Research and Technology 236, 17–28.

Rucker, R.B., Suttie, J.W., McCormick, D.B., 2001. Handbook of vitamins. CRC Press.

Rychlik, M., Englert, K., Kapfer, S., Kirchhoff, E., 2007. Folate contents of legumes determined by optimized enzyme treatment and stable isotope dilution assays. Journal of Food Composition and Analysis 20, 411–419. https://doi.org/10.1016/j.jfca.2006.10.006

Saini, R.K., Nile, S.H., Keum, Y.-S., 2016. Folates: chemistry, analysis, occurrence, biofortification and bioavailability. Food Research International 89, 1–13.

Scott, J., Rébeillé, F., Fletcher, J., 2000. Folic acid and folates: the feasibility for nutritional enhancement in plant foods. Journal of the Science of Food and Agriculture 80, 795–824.

Strandler, H.S., Patring, J., Jägerstad, M., Jastrebova, J., 2015. Challenges in the determination of unsubstituted food folates: impact of stabilities and conversions on analytical results. Journal of agricultural and food chemistry 63, 2367–2377.

Striegel, L., Chebib, S., Rychlik, M., Netzel, M.E., 2018. Improved stable isotope dilution assay for dietary folates using LC-MS/MS and its application to strawberries. Frontiers in chemistry 6, 11.

Suitor, C.W., Bailey, L.B., (2000). Dietary folate equivalents: Interpretation and application. Journal of the American Dietetic Association 100(1), 88-94.

Tscharntke, T., Clough, Y., Wanger, T.C., Jackson, L., Motzke, I., Perfecto, I., Vandermeer, J., Whitbread, A., 2012. Global food security, biodiversity conservation and the future of agricultural intensification. Biological conservation 151, 53–59.

Van Boekel, Martinus A.J.S, 2008. Kinetic Modeling of Reactions in Foods.

Verlinde, P.H., Oey, I., Lemmens, L., Deborggraeve, W.M., Hendrickx, M.E., Van Loey, A.M., 2010. Influence of Reducing Carbohydrates on (6 S)-5-Methyltetrahydrofolic Acid Degradation during Thermal Treatments. Journal of agricultural and food chemistry 58, 6190–6199.

Viberg, U., Jägerstad, M., Öste, R., Sjöholm, I., 1997. Thermal processing of 5-methyltetrahydrofolic acid in the UHT region in tWeihe presence of oxygen. Food chemistry 59, 381–386.

Waldron, K.W., Parker, M.L., Smith, A.C., 2003. Plant cell walls and food quality. Comprehensive Reviews in Food Science and Food Safety 2, 128–146.

Xue, S., Ye, X., Shi, J., Jiang, Y., Liu, D., Chen, J., Shi, A., Kakuda, Y., 2011. Degradation kinetics of folate (5-methyltetrahydrofolate) in navy beans under various processing conditions. LWT - Food Science and Technology 44, 231–238. https://doi.org/10.1016/j.lwt.2010.05.002

Fig 1: (a) Microtomography of cowpea seed. (b) Simplified geometrical representation of cowpea seed (ΩS) assuming a pseudo-ellipsoidal and symmetrical shape with specific dimensions (unit: 10-3m). ΩSW represents the soaking water domain. (c) Micrograph showing the gross morphology of cowpea seeds and (d) a magnified embryonic axis. C, cotyledon; E, embryonic axis; LM, leaf meristem; RM: root meristem. Scale bars = 1733 µm (c) and 831 µm (d).

Fig 2: Folate reaction scheme of the cowpea soaking-cooking process. Blue, green and orange lines represent enzymatic interconversion, chemical interconversion and thermal oxidation, respectively. Solid lines represent the reactions taken into account in the model and dashed lines the reactions that are not taken into account in the model.

Fig 3: (a) Immunostaining (highlighted by fluorescence) of 5-methyltetrahydrofolate in (a) root meristem of embryonic axis and (b) in the cotyledon. The diffuse background fluorescence is due to the autofluorescence of cells. Scale bars = 72 µm.

Fig 4: Predicted (lines) and experimental data (dots) concerning folic acid [PteGlu], 10-formylfolic acid [10-CHO-PteGlu], 5-formyltetrahydrofolate [5-CHO-H_4folate], 5-methyltetrahydrofolate [5-CH_3-H_4folate] and total folate [Total] concentrations (µg/100g db) in cowpea seeds and in the soaking water during soaking at 95 °C. Error bars represent standard deviations (n = 4).

Fig 5: Predicted (lines) and experimental data (dots) concerning folic acid [PteGlu], 10-formylfolic acid [10-CHO-PteGlu], 5-formyltetrahydrofolate [5-CHO-H_4folate], 5-methyltetrahydrofolate [5-CH_3-H_4folate] and total folate [Total] concentrations (µg/100g db) in cowpea seeds and in the soaking water during soaking at 60 °C. Error bars represent standard deviations (n = 4).

Fig 6: Predicted (lines) and experimental data (dots) concerning folic acid [PteGlu], 10-formylfolic acid [10-CHO-PteGlu], 5-formyltetrahydrofolate [5-CHO-H_4folate], 5-methyltetrahydrofolate [5-CH_3-H_4folate] and total folate [Total] concentrations (µg/100g db) in cowpea seeds and in the soaking water during soaking at 30 °C. Error bars represent standard deviations (n = 4).

Fig 7: Immunostaining of 5-methyltetrahydrofolate (fluorescent dots) in root meristems using Droit Zeiss 880 Laser Coherent Chameleon Ultra II Multiphoton microscope (left column) and using a confocal Zeiss LSM880 Airyscan microscope (right column). (a, b) Raw seeds (control), (c, d) after soaking at 60 °C for 1 h, after soaking at 95 °C for 0.25 h (e, f) and for 0.5 h (g, h). The

diffuse background fluorescence is due to the autofluorescence of cells. Arrows identify the location of 5-methyltetrahydrofolate in the intercellular spaces (f), and diffused outside the roots (g). Scale bars = 95 µm (left column) and 12.7 µm (right column).

Fig 8: Predicted algebraic residual, produced, diffused and degraded mass fraction kinetics for folic acid [PteGlu], 10-formylfolic acid [10-CHO-PteGlu], 5-formyltetrahydrofolate [5-CHO-H_4folate], 5-methyltetrahydrofolate [5-CH_3-H_4folate] and total folate [Total] in cowpea seed during the soaking-cooking process at 95 °C, 60 °C and 30 °C.

Table 1. Input parameters used in the 2D-axisymmetric reaction-diffusion model.

Table 2. Initial concentrations (µg/100g db) of folic acid [PteGlu] (C_1), 10-formylfolic acid [10-CHO-PteGlu] (C_2), 5-formyltetrahydrofolate [5-CHO-H_4folate] (C_3), 5-methyltetrahydrofolate [5-CH_3-H_4folate] (C_4), tetrahydrofolate [H_4folate] and total folate [Total] in whole seeds, in cotyledons and in the embryo. The embryo represents 2.3% of seed total mass.

Table 3. Estimated apparent diffusion coefficients (D_i, $m^2.s^{-1}$) and enzymatic or thermal degradation (*italics*) rate constants (k_{i,Ω_S}, s^{-1}) for each folate vitamer in cowpea seeds (Ω_S) and at different soaking-cooking temperatures (T) (mean values ± standard deviations determined with Monte-Carlo simulations: 200 sets).

Table 4. Absolute concentration of 5-methyltetrahydrofolate (5-CH_3-H_4folate) and 5-formyltetrahydrofolate (5-CHO-H_4folate (as a % of the intial concentration) in cowpea seeds by LC-MS/MS quantification (n=4) and image quantification (only 5-CH_3-H_4folate, n=2) after soaking at 60 °C for 1 h and cooking at 95 °C for 0.5 h.

Supplementary Table1: Nomenclature.

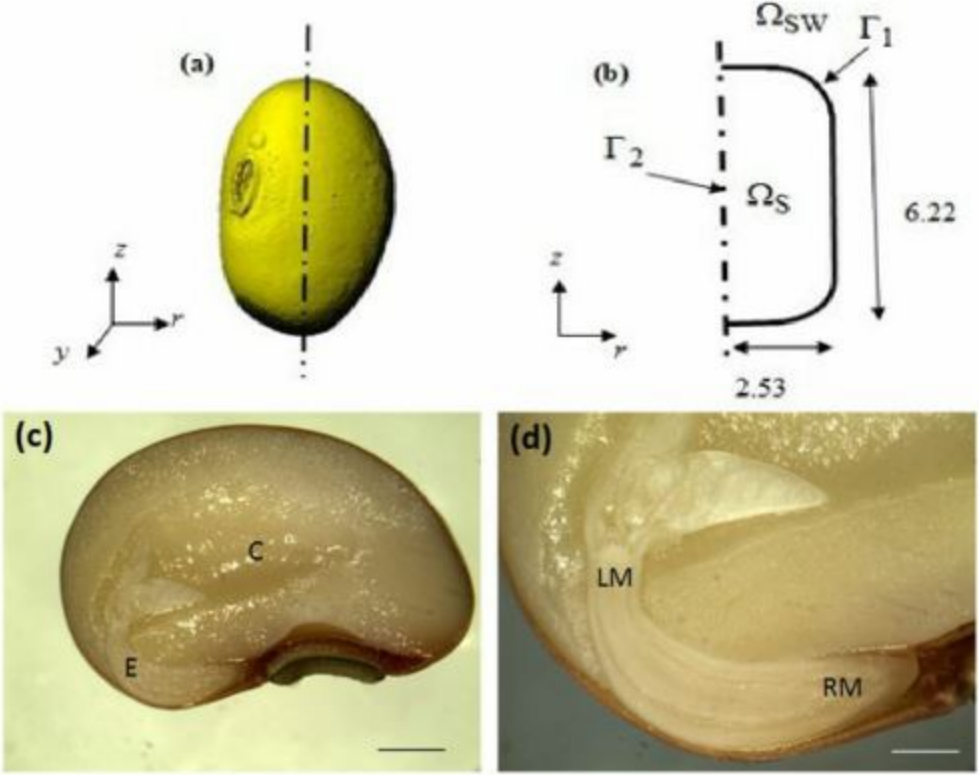
(a)
z
r
y
(b)
Ω_{SW}
Γ_1
Γ_2
Ω_S
6.22
2.53
z
r
(c)
C
E
(d)
LM
RM

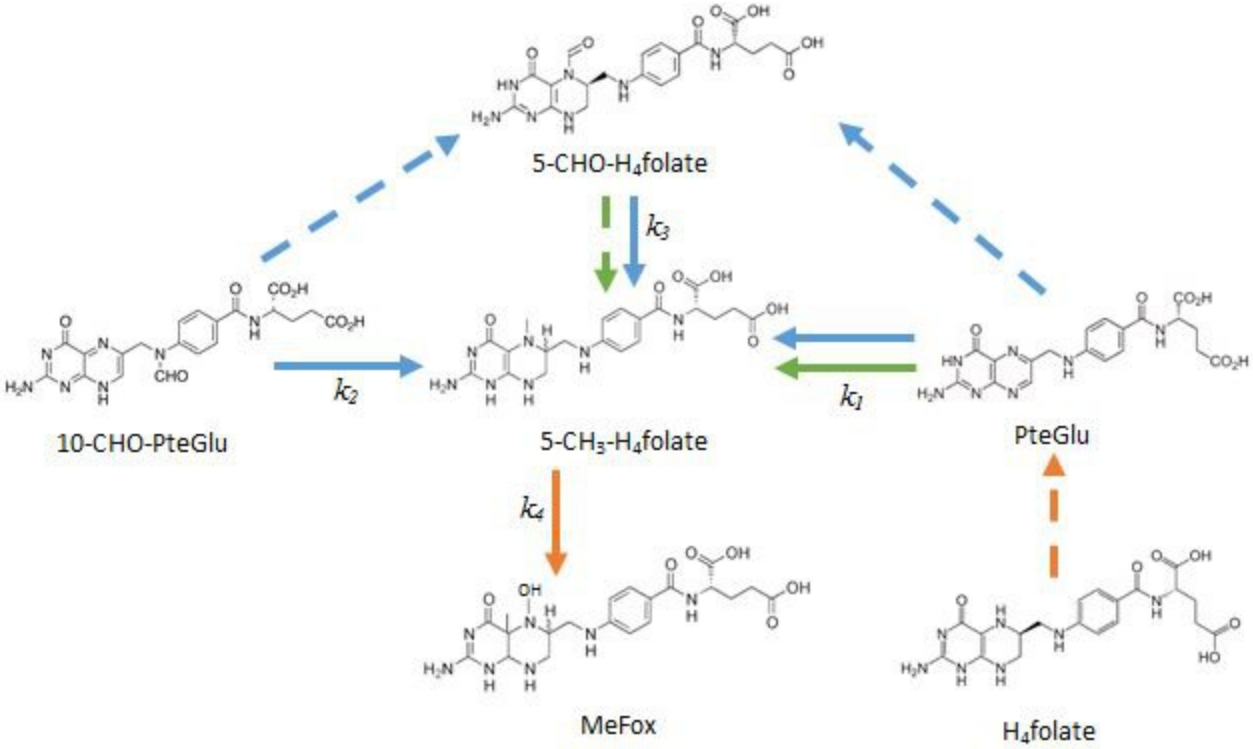

Enzymatic conversion

Chemical conversion

Themal oxidation

Solid lines : modeled

Dashed lines : Not modeled

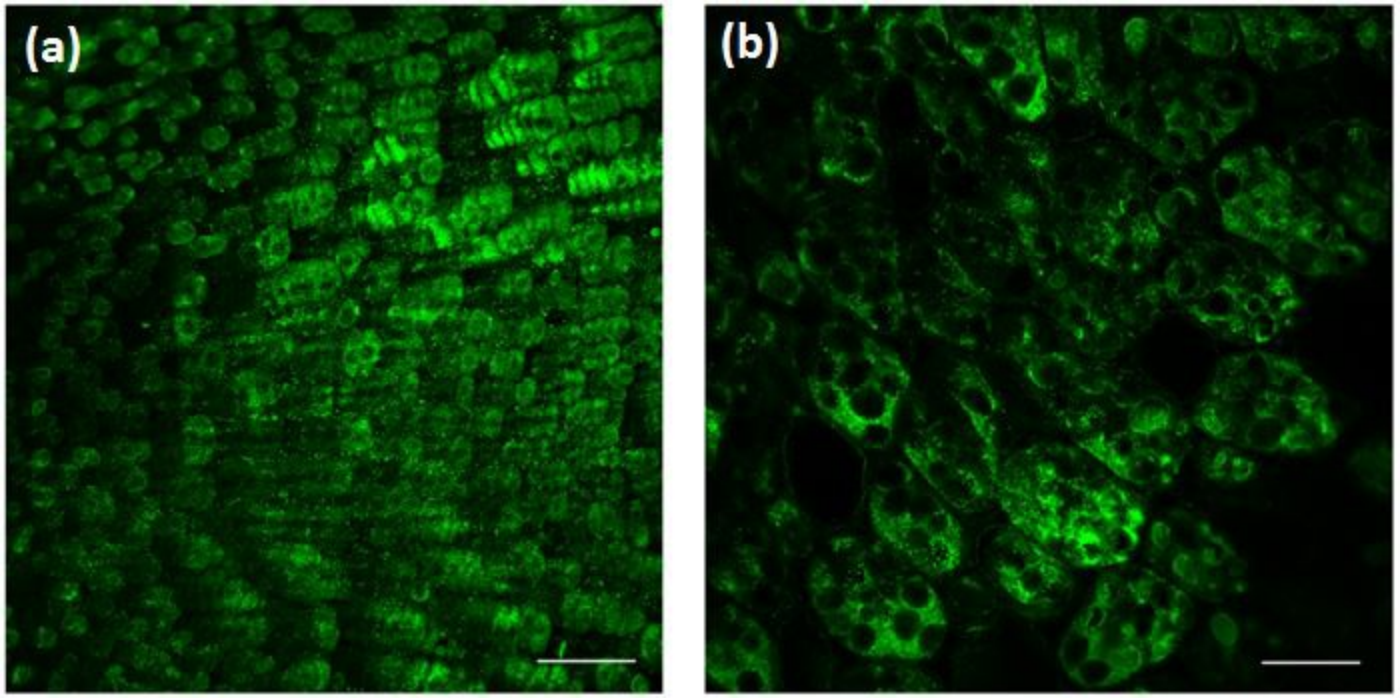
(a)
(b)

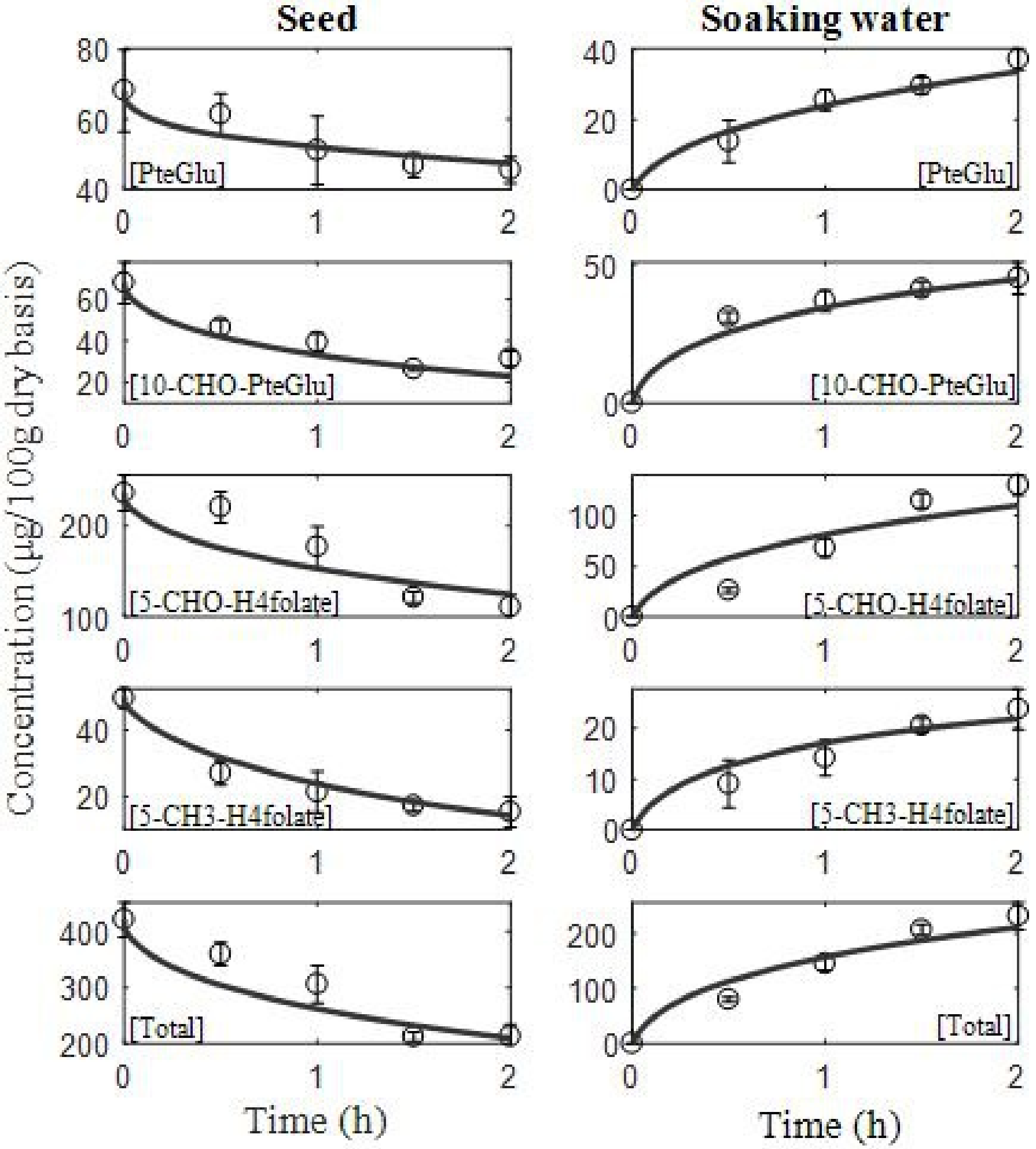
Seed
Soaking water
Concentration (μg/100g dry basis)
[PteGlu]
[10-CHO-PteGlu]
[5-CHO-H4folate]
[5-CH3-H4folate]
[Total]
Time (h)
Time (h)

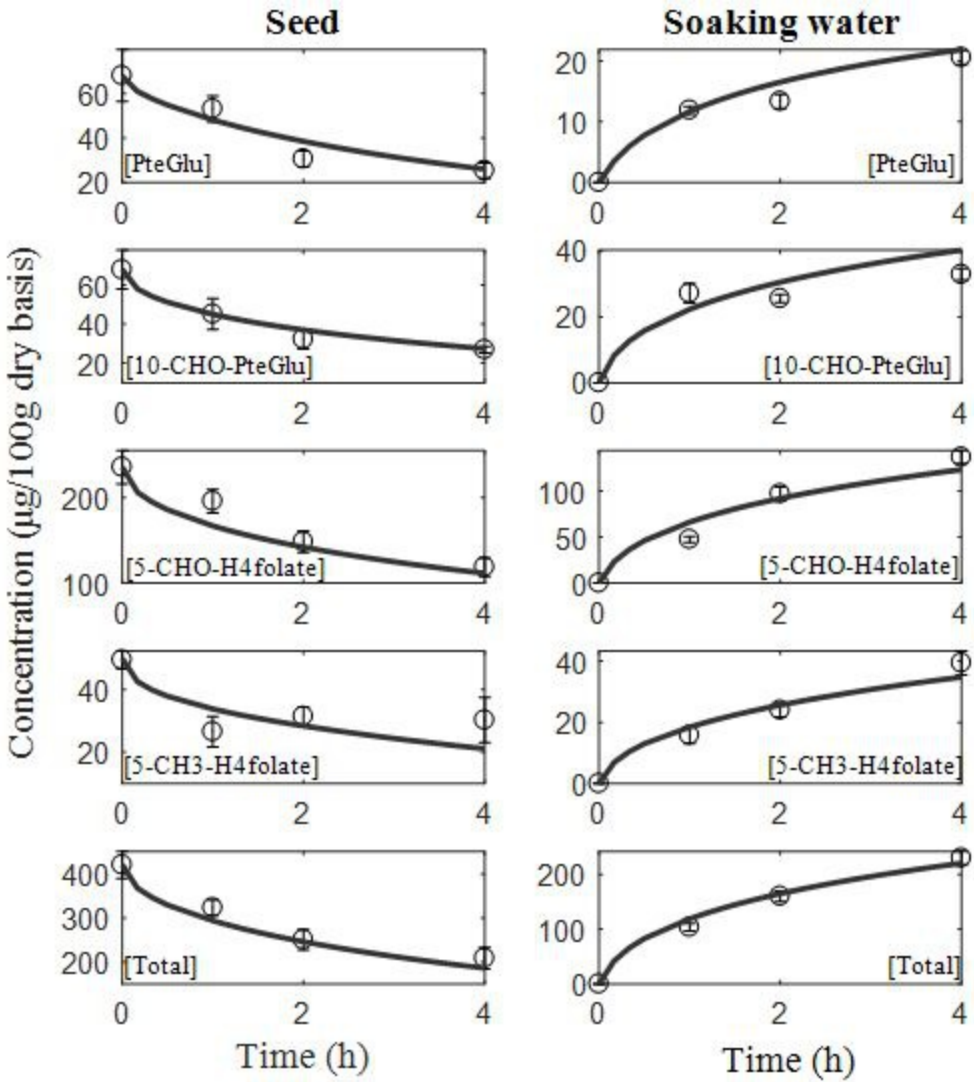
Seed
Soaking water
Concentration (µg/100g dry basis)
[PteGlu]
[10-CHO-PteGlu]
[5-CHO-H4folate]
[5-CH3-H4folate]
[Total]
Time (h)
Time (h)

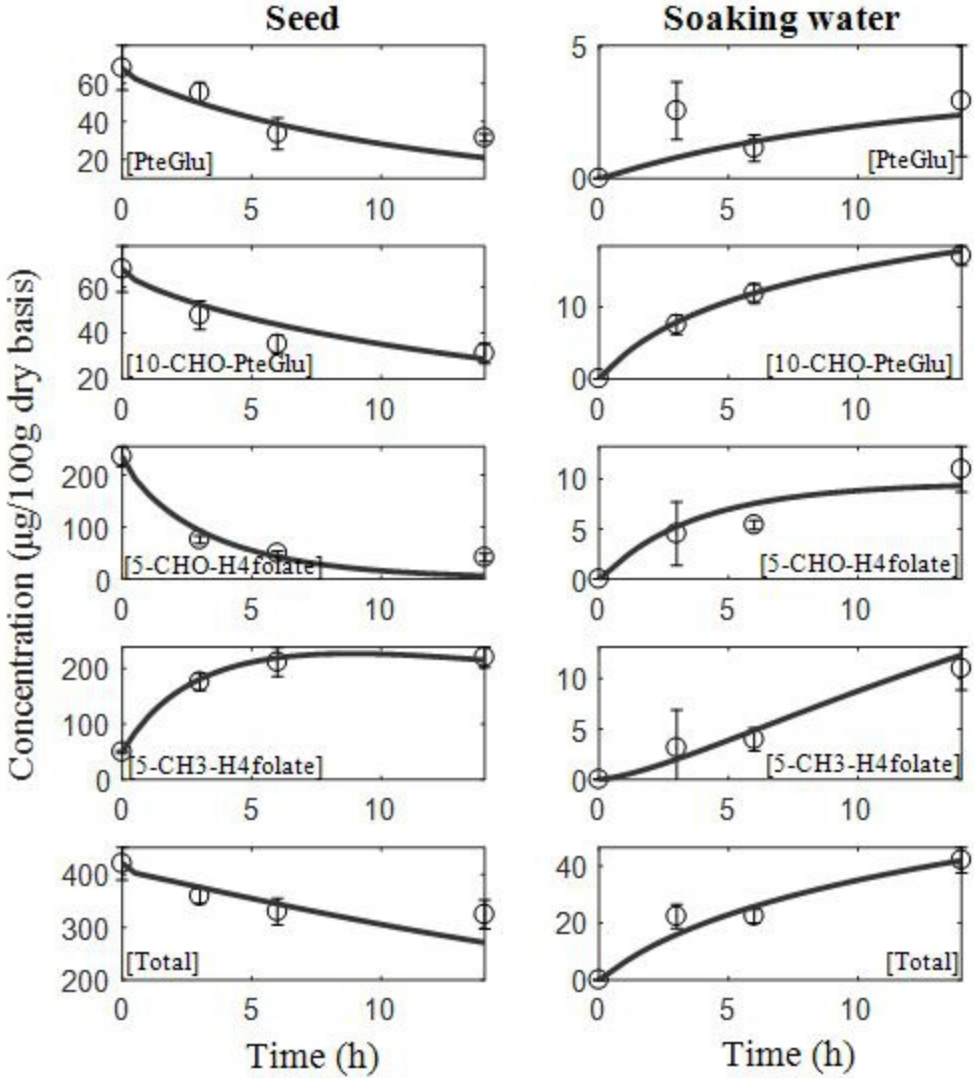
Seed
Soaking water
Concentration (µg/100g dry basis)
[PteGlu]
[10-CHO-PteGlu]
[5-CHO-H4folate]
[5-CH3-H4folate]
[Total]
Time (h)
Time (h)

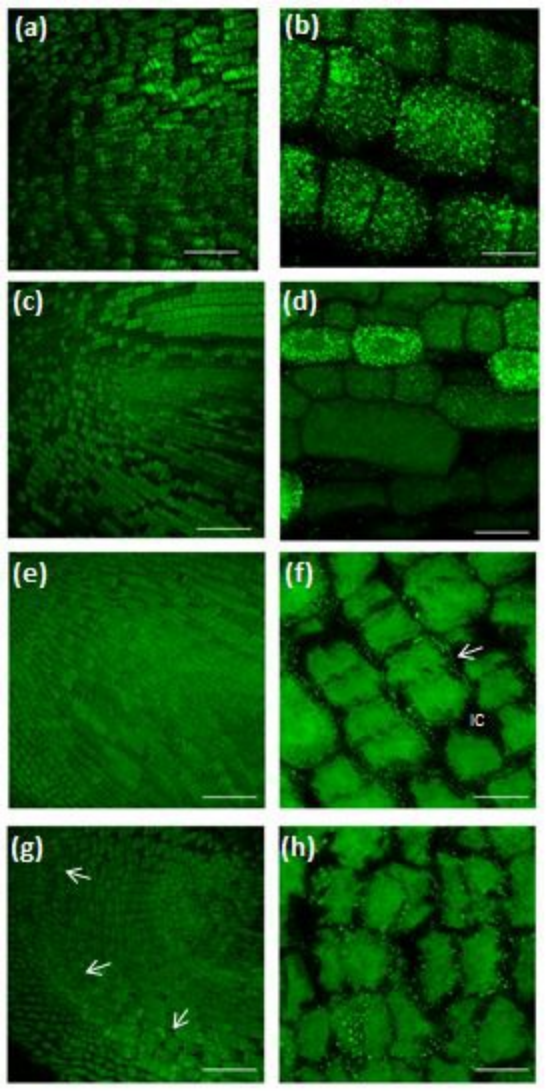
(a)
(b)
(c)
(d)
(e)
(f)
IC
(g)
(h)

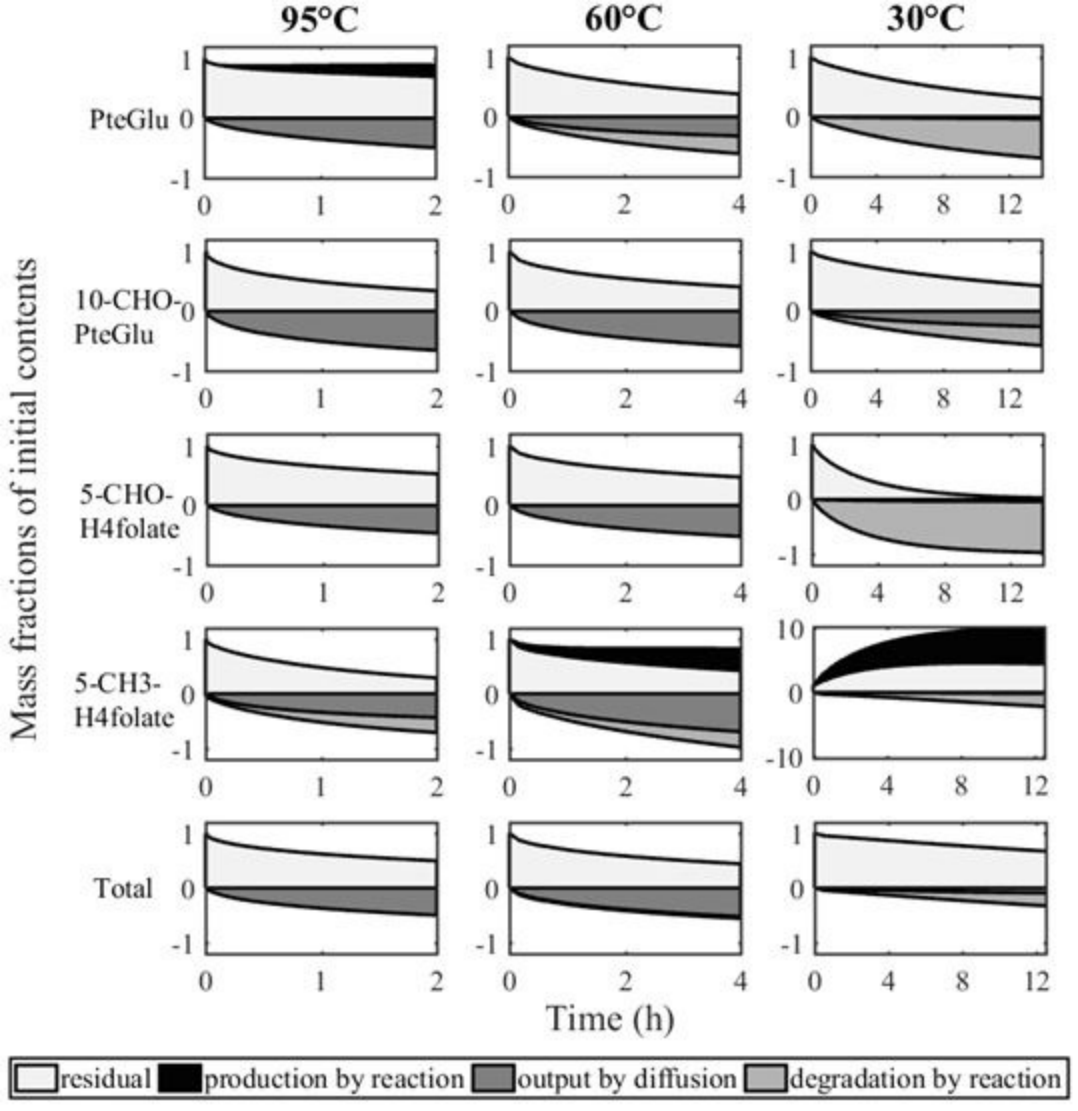
95°C
60°C
30°C
PteGlu
10-CHO-PteGlu
5-CHO-H4folate
5-CH3-H4folate
Total
Mass fractions of initial contents
Time (h)
residual
production by reaction
output by diffusion
degradation by reaction

Parameter	Value	Unit
$C_{1,\Omega_{S,0}}$	0.79×10^{-3}	kg.m^{-3}
$C_{2,\Omega_{S,0}}$	0.79×10^{-3}	kg.m^{-3}
$C_{3,\Omega_{S,0}}$	2.76×10^{-3}	kg.m^{-3}
$C_{4,\Omega_{S,0}}$	0.58×10^{-3}	kg.m^{-3}
ρ_{DM}^{0}	1302	kg.m^{-3}
V_{Ω_S}	1.09×10^{-7}	m^3

Vitamers	Initial concentrations (µg/100g db)		
	Seeds	**Cotyledons**	**Embryonic axis**
$[PteGlu](C_1)$	68.1 ± 11.7	70.8 ± 7.2	98.4 ± 11.0
$[10-CHO-PteGlu](C_2)$	67.9 ± 10.0	69.7 ± 3.4	64.0 ± 2.9
$[5-CHO-H_4folate](C_3)$	235.6 ± 19.4	239.4 ± 11.9	752.9 ± 33.8
$[5-CH_3-H_4folate](C_4)$	49.5 ± 2.9	28.4 ± 2.4	71.9 ± 2.7
$[H_4folate]$	13.8 ± 2.2	3.1 ± 0.7	24.4 ± 1.8
Total	434.9 ± 20.8	411.3 ± 7.2	1012 ± 35.0

Vitamers	T(°C)	$D_i \times 10^{11} (m^2 s^{-1})$	$k_{i,\Omega_S} \times 10^5 (s^{-1})$	RMSE*	
				In seed (S)	In soaking water (SW)
Folic acid (i = 1)	30	0.010 ± 0.001	2.21 ± 0.04	8.9	1.3
	60	0.81 ± 0.02	3.73 ± 0.06	7.2	1.4
	95	3.12 ± 0.06	0	7.3	3.5
10-formyl-folic acid (i = 2)	30	0.181 ± 0.003	0.81 ± 0.01	8.3	1.3
	60	2.93 ± 0.05	0	6.3	5.2
	95	7.94 ± 0.16	0	6.6	4.4
5-formyl-H_4folate (i = 3)	30	0.026 ± 0.001	8.0 ± 0.12	23.0	2.4
	60	2.12 ± 0.04	0	20.1	12.4
	95	3.23 ± 0.05	0	29.3	19.9
5-methyl-H_4folate (i = 4)	30	0.014 ± 0.002	1.11 ± 0.02	17.1	1.4
	60	3.52 ± 0.07	3.39 ± 0.06	7.1	3.3
	95	3.63 ± 0.06	7.73 ± 0.14	4.2	3.4

*RMSE: Root mean square error between experimental and predicted concentrations in $(mg/100\,kg\ db)$.

Technic of quantification	Vitamer	Quantification in %	
		60°C_1h	95°C_30min
By immunostaining	5-CH_3-H_4folate	52 ± 26	43 ± 8
By LC/MS	5-CH_3-H_4folate	54 ± 19	55 ± 13
	5-CHO-H_4folate	83 ± 7	93 ± 8